Particle Accelerators
1976, Vol. 7, pp. 223–243

THEORY OF RF ION BEAM CHOPPERS WITH FRINGING FIELDS

JOHN J. LIVINGOOD

Argonne National Laboratory, Argonne, Illinois 60439, USA

(*Received June 17, 1976*)

If fringing fields are neglected, it is known that the transmitted beam of zero slope suffers a finite lateral displacement (thus necessitating a slit wider than the beam's diameter to ensure passage of all ions) and that an increasing divergence is introduced as the beam is more and more cut off by the slit jaws, provided an arbitrary value is assigned to the chopper's angular length ϕ. It is here shown that, in addition, there is an unwanted fully transmitted beam of finite slope. These same conclusions hold in the realistic case with fringing fields, these being approximated by linear ramps of angular length ε. But if certain *particular* values of ϕ are employed with any given ε, then the zero slope beam also has zero lateral displacement and there is no fully passed beam of finite slope. Under special conditions and at the expense of much higher voltage, the divergence introduced by chopping can be made to approach zero.

INTRODUCTION

A chopper converts a continuous stream of charged particles into separated short pulses by sweeping the beam up and down, say, across a slit in a barrier. This motion is caused by passing the beam between two plane electrodes between which there is an alternating electric field. A plot of transmitted intensity vs time is triangular. Ions near cut-off have vertical divergence but it is of paramount importance for downstream apparatus that those at the peak should emerge with zero vertical slope. Because the chopper has finite length, the transit time throught it is finite, so no particles traverse it in a straight path. In the general case where the length is arbitrary, there exists a phase of the field at entry such that the curved path results in the peak current emerging with the desired zero slope but unfortunately shifted up or down by a finite amount. If partial interception is not to occur, the downstream slit must be wider than the beam's diameter, thus requiring a larger field (to bring about the wanted interception of ions entering earlier and later) than if the zero-slope beam had been on the axis.

A major objective of this article is to show that if the chopper be one of several *particular* lengths, then the zero slope beam also enjoys zero displacement.

The usual analysis of a chopper assumes (in the interest of simplicity) an abrupt drop of the field to zero at the physical ends of the chopper. This is unwarranted; there is a rapidly decaying fringing field that extends beyond the real edges. A second major purpose of this paper is to investigate the effects of such fringing fields.

A chopper is inefficient, since the shorter the passed pulse, the greater is the fraction of the total beam that is intercepted. A more complicated "buncher" device is hence often used to slow down early ions and to accelerate those that reach it later, so at a downstream point all are more or less bunched together The bunch, however, has leading and lagging tails which a chopper can remove to bring about a more favorable quasi-rectangular pulse. Some deviation from predicted chopper action will occur since the buncher introduces an energy spread which is not considered in the present analysis.

THE FRINGING FIELD

To describe this we make use of the parametric equations[1] for a semi-infinite parallel plate capacitance in which there is a dc field:

$$\begin{aligned} E/E_o &= 1/(1 + u) \\ z &= (1 + u + \ln u)G/2\pi, \end{aligned} \tag{1}$$

where E is the midplane field at a distance z beyond the capacitance and E_o is its value well inside, G being the separation of the plates. A plot of E/E_o vs z/G (derived by assigning values to u) is

shown by the curved line in Figure 1. The tail of the curve goes to infinity.

The fringing field arises from lines of force running from the top surface of the upper plate to the bottom surface of the lower one. If the structure extends to infinity to the left, on the right there will be lines crossing the midplane out to $z = \infty$. One particular line, originating at a distance $S/2$ from the open end, at point A, will cross the midplane at point B, located a distance z_1' from this end. Now if the capacitance has a finite length S, all the lines originating to the left of point A will now curve the other way in order to supply the fringe field at the left end. Point B moves further to the right, to a distance $z_1 > z_1'$, because there are now no lines to the right of B exerting a force to the left (adapting Faraday's picture) but there is the tension in the line from A to B, so the value of z_1 results from an

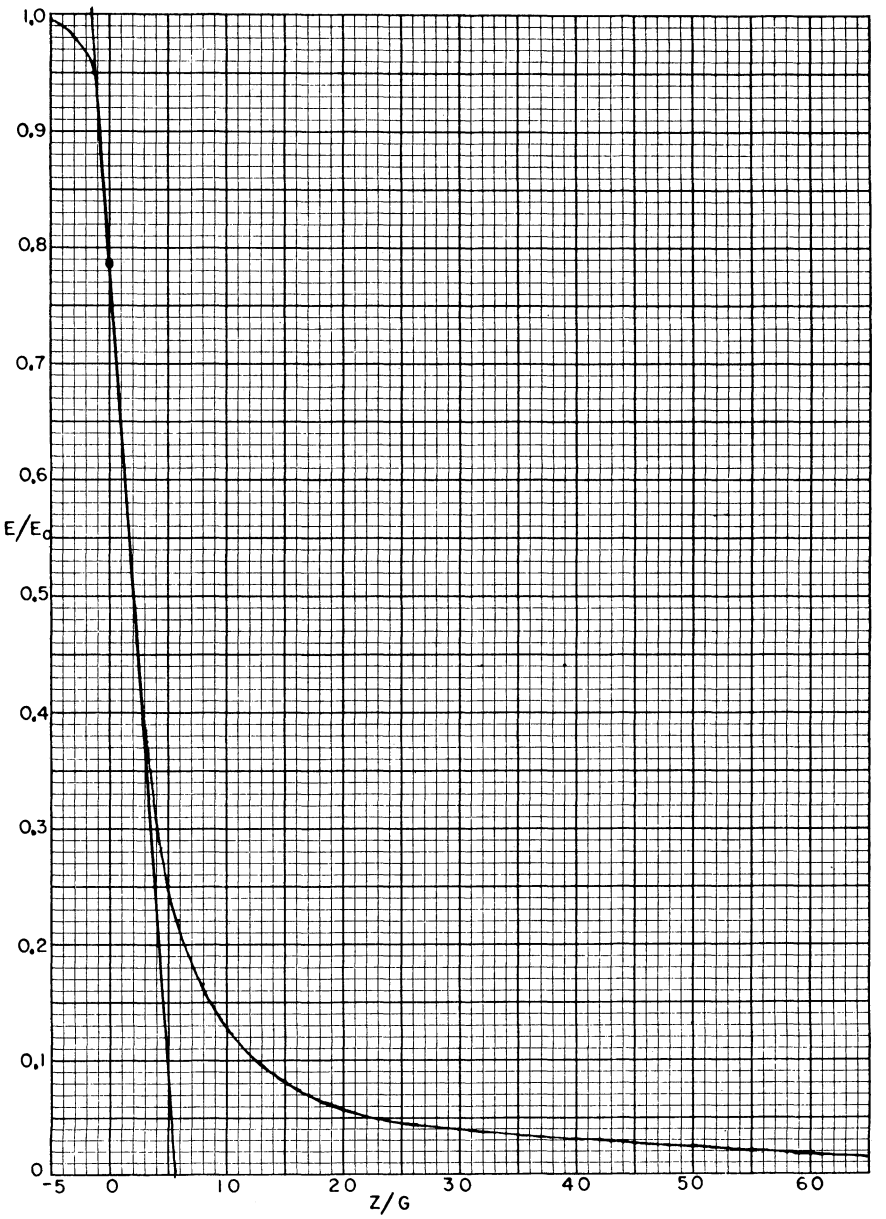

FIGURE 1 The curved line represents the fractional fringing field of a semi-infinite capacitance as a function of the ratio of distance to gap. The straight line is the approximate fringe field of a finite chopper.

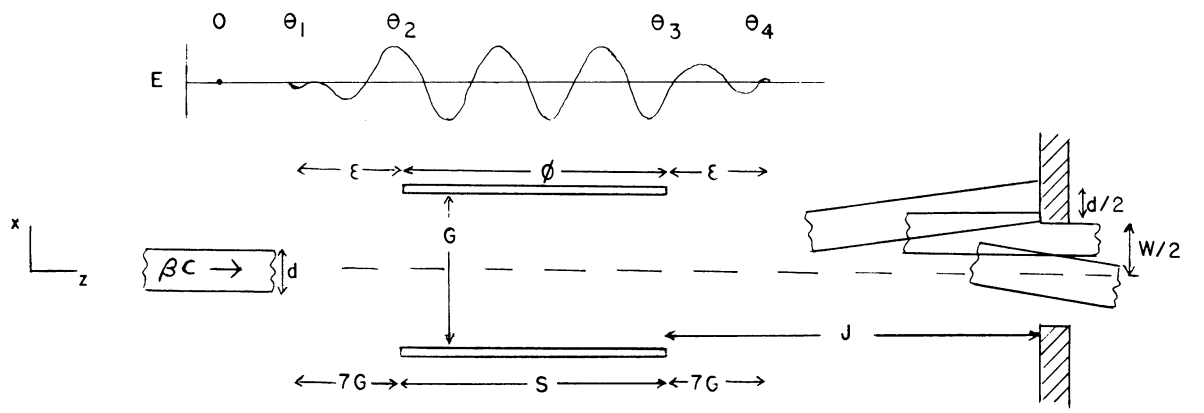

FIGURE 2 Schematic picture of a chopper of idealized length S and fringe fields of length $7G$, with indication of entering beam and three emergent beams; one just intercepted, a second with zero slope but partially cut off, the third being the diagonal, fully passed beam with finite slope. Not to scale.

equilibrium of forces of tension and repulsion. Since there is now a last line to the right, we may conclude that the fringing field of a finite unit does not have appreciable value to infinity; hence the area under the curve of Figure 1, as applied to a finite chopper, may be taken as finite. The same conclusions hold when the field is alternating, E_o then being the amplitude.

A truly rigorous analysis would determine the magnitude of z_1, followed by integration of the force in the fringing region. But since this force is not describable by a simple analytic function, we will be content with an approximate treatment. We replace the curve of Figure 1 by the straight line that best fits the steepest descent, neglecting the small change in slope arising from the reduced number of lines to the right and by ignoring the now finite tail and the small curved region at the top. The intercepts at E/E_o equal to one and zero are seen to be $z_1/G = -1.5$ and 5.5, thus giving a total span in z_1/G of 7, in this approximation of a linear ramp field. Although the performance calculated on this basis will not be quite correct, it will be nearer the truth than if the fringe fields are entirely neglected.

It is important to notice that the ramp penetrates within the chopper by the distance $1.5G$ at each end. The idealized region of length S, over which the field will be assumed to be uniform in space, is a fictitious realm that is shorter, by $3G$, than the true length S_{true}. This latter will not be mentioned henceforth and it should be remembered that we have

$$S_{\text{true}} = S + 3G. \tag{2}$$

We assume a uniform density of particles of common speed βc and that the beam has no divergence. Time and phase are measured from a null in the sinusoidal field. (See Figure 2.) Let the ramp be first encountered at $\theta_1 = \omega t_1$ while the chopper is reached at $\theta_2 = \omega t_2$ ($\omega = 2\pi$ freq.). Let

$$1/\alpha = t_2 - t_1 = z_1/\beta c = 7G/\beta c. \tag{3}$$

Define ε as

$$\begin{aligned} \varepsilon &= \omega/\alpha = \omega(t_2 - t_1) = \theta_2 - \theta_1 \\ &= 7\omega G/\beta c, \end{aligned} \tag{4}$$

so that ε is the angular length of each fringe field in radians. The extent of these fields and their phase when a particle enters them will have a strong influence on the slope and lateral displacement at the final emergence.

There may be legitimate differences of opinion on the validity of the factor 7 in Eq. (4), but the following analysis is in terms of ε, irrespective of what number seems best.

THE EQUATIONS OF MOTION

The entrance ramp is described as

$$E = E_o\alpha(t - t_1)\sin \omega t, \tag{5}$$

where E_o is the field's amplitude inside the chopper. When $t = t_1$ then $E = 0$, and when $t = t_2$ then $E = E_o \sin \omega t$, by virtue of Eq. (3). The equation of transverse motion for a particle of mass M and charge Q is

$$Md^2x/dt^2 = QE_o\alpha(t - t_1)\sin \omega t. \tag{6}$$

Integration between t_1 and t_2 yields the following for the transverse velocity and displacement at entry into the chopper.

$$v_2 = KE_o\omega\{\cos\theta_1[(1/\varepsilon)\sin\varepsilon - \cos\varepsilon] + \sin\theta_1[\sin\varepsilon - (1/\varepsilon)(1 - \cos\varepsilon)]\} \quad (7)$$

$$x_2 = KE_o\{\cos\theta_1[(2/\varepsilon)(1 - \cos\varepsilon) - \sin\varepsilon] + \sin\theta_1[(2/\varepsilon)\sin\varepsilon - \cos\varepsilon - 1]\}, \quad (8)$$

where

$$K = Q/M\omega^2 = Zc^2/(NM_oc^2\omega^2) = Zc^2/(9.31 \times 10^8\, N\omega^2) = 9.66 \times 10^{11} Z/(N\omega^2)(\text{cm}^2/\text{volt}), \quad (9)$$

where Z is the number of electronic charges and N is the number of nucleons. The upper limit θ_2 has been expressed in terms of θ_1 through the relation $\theta_2 - \theta_1 = \varepsilon$.

The chopper itself, of fictional length S, is traversed between $\theta_2 = \omega t_2$ and $\theta_3 = \omega t_3$, with $\theta_3 - \theta_2 = \phi$, where

$$\phi = \omega S/\beta c \quad (10)$$

is the angular length of the chopper, in radians. This analysis is largely concerned with the proper choice of ϕ, and when this has been made the length S may be calculated from Eq. (10).

In the chopper we have

$$Md^2x/dt^2 = QE_0 \sin\omega t, \quad (11)$$

and integration between t_2 and t_3 gives the transverse velocity and displacement at the exit from the chopper as

$$v_3 = KE_o\omega\{\cos\theta_1[\sin\phi\sin\varepsilon - \cos\phi\cos\varepsilon + (1/\varepsilon)\sin\varepsilon] + \sin\theta_1[\cos\phi\sin\varepsilon + \sin\phi\cos\varepsilon - (1/\varepsilon)(1 - \cos\varepsilon)]\} \quad (12)$$

$$x_3 = KE_o\{\cos\theta_1[-\cos\phi\sin\varepsilon - \sin\phi\cos\varepsilon + (\phi/\varepsilon)\sin\varepsilon + (2/\varepsilon)(1 - \cos\varepsilon)] + \sin\theta_1[\sin\phi\sin\varepsilon - \cos\phi\cos\varepsilon - (\phi/\varepsilon)(1 - \cos\varepsilon) + (2/\varepsilon)\sin\varepsilon - 1]\} \quad (13)$$

The complexity of these arises because the initial and final phases have been given in terms of the entrance phase θ_1, using $\theta_3 - \theta_2 = \phi$ and $\theta_2 - \theta_1 = \varepsilon$.

The final ramp field extends from $\theta_3 = \omega t_3$ to $\theta_4 = \omega t_4$, with $\theta_4 - \theta_3 = \varepsilon$. It is described as

$$E = E_o[1 - \alpha(t - t_3)]\sin\omega t. \quad (14)$$

This gives $E_o \sin\omega t$ when $t = t_3$ and zero when $t = t_3 + z_1/\beta c = t_3 + 1/\alpha$. The integration is no more difficult than before, but because of the desire to again express the limits in terms of θ_1, the final expressions for v_4 and x_4 are extremely complicated. It is convenient to introduce a number of abbreviations. Let

$$A = (1 - 2\cos\varepsilon)\sin\varepsilon \quad (15)$$

$$B = \cos^2\varepsilon - \sin^2\varepsilon - \cos\varepsilon \quad (16)$$

$$C = \sin\varepsilon + \varepsilon\cos\varepsilon + 2B/\varepsilon \quad (17)$$

$$D = \cos\varepsilon - \varepsilon\sin\varepsilon + 2A/\varepsilon \quad (18)$$

$$p = [A\cos\phi - B\sin\phi + \sin\varepsilon]/\varepsilon \quad (19)$$

$$q = [-B\cos\phi - A\sin\phi - (1 - \cos\varepsilon)]/\varepsilon \quad (20)$$

$$m = C\cos\phi + D\sin\phi + (\phi/\varepsilon)\sin\varepsilon + (2/\varepsilon)(1 - \cos\varepsilon) \quad (21)$$

$$n = D\cos\phi - C\sin\phi - (\phi/\varepsilon)(1 - \cos\varepsilon) + (2/\varepsilon)\sin\varepsilon - 1. \quad (22)$$

The transverse velocity and displacement on leaving the exit fringe field are then

$$v_4 = KE_o\omega(p\cos\theta_1 + q\sin\theta_1) \quad (23)$$

$$x_4 = KE_o(m\cos\theta_1 + n\sin\theta_1). \quad (24)$$

To obtain an output beam of zero slope, Eq. (23) must vanish. This means that such ions entered the first ramp at the phase angle θ_{10v} given by

$$\tan\theta_{10v} = \frac{p}{-q} = \frac{A\cos\phi - B\sin\phi + \sin\varepsilon}{B\cos\phi + A\sin\phi + 1 - \cos\varepsilon}. \quad (25)$$

The subscript $10v$ implies the entry phase which gives zero value to v_4. When $\varepsilon = 7\omega G/\beta c$ is known and when $\phi = \omega S/\beta c$ has been chosen, Eq. (25) may be evaluated and θ_{10v} may be used for θ_1 in Eq. (24) to find the lateral displacement, at the exit from the final ramp, for those ions which there have zero slope. Random but reasonable choices of ε and ϕ can give x_4/KE_o up to several tens.

INTERCEPTION OF IONS AND PULSE LENGTH

Ions entering the first ramp at any phase other than θ_{10v} will, in general, leave the final ramp with a slope and displacement that are both finite. Hence

the displacement at the slit jaws, at distance J beyond the chopper, can be enough for total interception. Let the phase shifts (to either side of θ_{10v}) that are needed to just cause cut-off be $\Delta\theta_a$ and $-\Delta\theta_b$. The absolute values of these will not be the same, since if the zero-slope beam is displaced, say, below the axis, a lesser change in entry phase is needed to direct it to the lower jaw than is needed to direct it to the upper one. The two entry phases for cut-off are then

$$\theta_{1co} = \theta_{10v} \pm \Delta\theta_{a,b} \tag{26}$$

where the upper sign goes with $\Delta\theta_a$ and the lower with $\Delta\theta_b$. As a convenience in writing let us define

$$\sigma = \sin\theta_{10v} \tag{27}$$

$$\kappa = \cos\theta_{10v}. \tag{28}$$

Then

$$\begin{aligned}\sin\theta_{1co} &= \sigma\cos\Delta\theta_{a,b} \pm \kappa\sin\Delta\theta_{a,b} \\ &= \sigma \pm \kappa\Delta\theta_{a,b}\end{aligned} \tag{29}$$

$$\begin{aligned}\cos\theta_{1co} &= \kappa\cos\Delta\theta_{a,b} \mp \sigma\sin\Delta\theta_{a,b} \\ &= \kappa \mp \sigma\Delta\theta_{a,b}\end{aligned} \tag{30}$$

since $\Delta\theta_{a,b} \ll 1$. The transverse speed and displacement v_4 and x_4 for entry phases θ_{1co} are given by expressions like Eqs. (23) and (24) but wherein θ_1 is replaced by θ_{1co} of Eq. (26).

The displacement x_J at the jaws, distant J beyond the chopper, is

$$x_J = x_4 + (J - r)\text{slope} = x_4 + (J - r)v_4/\beta c. \tag{31}$$

Here the length of the ramp field is written as

$$r = 7G. \tag{32}$$

For v_4 and x_4 we employ Eqs. (23) and (24), in which θ_1 is replaced by θ_{1co} so as to refer to the just-intercepted beams. Equation (31) becomes

$$x_J = KE_oH \tag{33}$$

where

$$\begin{aligned}H = {} & m\cos\theta_{1co} + n\sin\theta_{1co} + (\omega/\beta c)(J - r) \\ & \times (p\cos\theta_{1c0} + q\sin\theta_{1co}).\end{aligned} \tag{34}$$

In this we use Eqs. (29) and (30), and rearrange terms to obtain

$$H_{a,b} = X \mp \Delta\theta_{a,b}Y, \tag{35}$$

where

$$X = m\kappa + n\sigma + (\omega/\beta c)(J - r)(p\kappa + q\sigma) \tag{36}$$

$$Y = m\sigma - n\kappa + (\omega/\beta c)(J - r)(p\sigma - q\kappa). \tag{37}$$

To obtain equal up and down deflections we need $x_{Jb} = -x_{Ja}$, so by Eq. (33) we find that

$$\Delta\theta_b = \Delta\theta_a - 2X/Y. \tag{38}$$

Irrespective of the relative sizes of $\Delta\theta_a$ and $\Delta\theta_b$, their sum is the total phase shift from cut-off on one jaw to cut-off on the other, the corresponding time interval being T. That is

$$\Delta\theta_a + \Delta\theta_b = \omega T. \tag{39}$$

From this and Eq. (38) it follows that

$$\Delta\theta_{a,b} = \omega T/2 \pm X/Y \tag{40}$$

and using Eq. (35) we find that

$$H_{a,b} = \mp\omega TY/2 \tag{41}$$

the upper (lower) sign going with $H_a(H_b)$. The total deflection from bare cut-off on one jaw to that on the other is $W + d$, where W is the slit width and d is the beam's diameter. Hence

$$W + d = KE_o(H_a - H_b) = -KE_o\omega TY \tag{42}$$

so that

$$E_oT = \frac{-(W + d)}{K\omega Y}. \tag{43}$$

Substitute for K from Eq. (9), for Y from Eq. (37) and write $E_o = V_o/G$, where V_o is the peak potential across the gap. This gives

$$V_oT = \frac{1.04 \times 10^{-12}G\omega N(W + d)}{Z[\mu - (\omega/\beta c)(J - 7G)v]}, \tag{44}$$

where

$$\mu = n\kappa - m\sigma = n\cos\theta_{10v} - m\sin\theta_{10v} \tag{45}$$

$$v = p\sigma - q\kappa = p\sin\theta_{10v} - q\cos\theta_{10v}. \tag{46}$$

All lengths are in centimeters. Recall that θ_{10v} is given by Eq. (25) in terms of known ε and chosen ϕ. From Eq. (44) we may calculate the peak voltage V_o for any desired pulse duration T, subject to a limitation which will be described later.

The denominator of Eq. (44) merits discussion. The lateral displacement at the exit from the final ramp is given by Eq. (24) which at cut-off reads

$$x_4 = KE_o(m\cos\theta_{1co} + n\sin\theta_{1co}). \tag{47}$$

Using Eqs. (29), (30) and (45) this becomes

$$x_4 = KE_o(m\kappa + n\sigma) \pm KE_o\Delta\theta_{a,b}\mu. \tag{48}$$

Hence μ measures the displacement of the cut-off paths at the exit from the second ramp in terms of

the entry phase for zero slope and in terms of the shifts, from that phase, which are necessary for interception on the jaws. The slope at cut-off is

$$\begin{aligned}\text{Slope}_{co} &= v_4/\beta c \\ &= (p\cos\theta_{1co} + q\sin\theta_{1co})KE_o\omega/\beta c \quad (49)\end{aligned}$$

by the use of Eq. (23) written for cut-off. Equations (29) and (30) convert this to

$$\begin{aligned}\text{Slope}_{co} &= (p\kappa + q\sigma)KE_o\omega/\beta c \\ &\quad \mp \Delta\theta_{a,b}(p\sigma - q\kappa)KE_o\omega/\beta c.\end{aligned}$$

In this the first term is $v_4/\beta c$ for entry phase θ_{10v} [see Eqs. (23), (27) and (28)] so this term vanishes and we obtain

$$\text{Slope}_{co} = \mp \Delta\theta_{a,b}\nu KE_o\omega/\beta c \quad (50)$$

by virtue of Eq. (46). Thus ν is proportional to the slope of the cut-off beam on leaving the final ramp. Calculation of this slope should be made for both $\Delta\theta_a$ and $\Delta\theta_b$ as given by Eq. (40), and the larger slope should be used in quoting the divergence introduced by the chopper.

Returning to Eq. (44) we see that if μ and ν are of opposite sign then V_oT is least, there being an upward (downward) displacement on leaving the ramp coupled with an upward (downward) slope so as to cause interception on the upper (lower) jaw. But when μ and ν have the same sign, V_oT is much greater, an upward displacement being associated with a downward slope to cause cut-off on the lower jaw, and conversely. As ν decreases so does the slope and when $\nu = 0$ we might expect the ideal chopper, since if μ is finite and if V_o is adequate, the beam would move from cut-off to full transmission to cut-off, yet always with zero slope, the lever arm $J - 7G$ then being immaterial. This situation will be discussed at greater length further on.

THE MINIMUM GAP AND PULSE

The shortest pulse occurs when V_o has been made so large that the lateral displacement inside the chopper is great enough to cause the ions to strike it. The largest internal displacement, $x_{\max}$, is determined by inspection of a plot of the interior path, obtained by use of Eq. (13) for x_3/KE_o. This is solved with constant ε (and hence constant G), and constant entrance phase θ_1 but with ϕ increasing, by steps, from zero to its full value, as though we were finding the exit displacement from a chopper of increasing length. This tedious method of obtaining $x_{\max}$ is necessary because equating $dx_3/d\phi$ to zero leads to an expression which is not solvable for ϕ. With K and G known and with V_o obtained from Eq. (44) (for a given T), we find $x_{\max} = (x_{\max}/KE_o)KE_o$. The least permissible gap (when the ions graze the chopper) is

$$G_{\min} = 2(x_{\max} + d/2), \quad (51)$$

and when this becomes as large as G, the lower limit of T has been reached. To obtain a shorter pulse it is necessary to increase G (and hence ε).

In the general case there are two relevant interior paths to compute and inspect for $x_{\max}$; those for cut-off on the upper and lower jaws, with $\theta_1 = \theta_{10v} \pm \Delta\theta_{a,b}$ where $\Delta\theta_{a,b}$ are given by Eq. (40). When $\Delta\theta_{a,b}$ are small compared with θ_{10v} they may be neglected without causing serious error in $G_{\min}$.

THE REQUIRED SLIT WIDTH

Because the zero-slope beam is displaced above or below the midplane (in the case of arbitrary ϕ), it will partly be intercepted by the slit jaw unless the slit be wider than the beam's diameter at that point. (The slit must straddle the midplane symmetrically, since all deflections change sign during each cycle.) To avoid partial interception (see Figure 2) we must have $x_4 + d/2 = W/2$ or

$$W = 2x_4 + d = 2KE_o(m\kappa + n\sigma) + d \quad (52)$$

via Eq. (24) (written to describe the zero-slope beam) and by use of Eqs. (27) and (28). Thus W depends on E_o, and E_o may be found only through use of the cut-off relation of Eq. (33), here written as

$$(W + d)/2 = KE_oH. \quad (53)$$

Eliminating E_o from these two expressions yields

$$\frac{W}{d} = \frac{H + (m\kappa + n\sigma)}{H - (m\kappa + n\sigma)}. \quad (54)$$

We now express H in terms of Eqs. (35), (36) and (37), and after some manipulation we find that

$$W/d = 1 + \eta, \quad (55)$$

where

$$\eta = \frac{2(m\kappa + n\sigma)}{(J - r)(p\kappa + q\sigma)\omega/\beta c \mp \Delta\theta_{a,b}[-\mu + \nu(J - r)\omega/\beta c]}. \quad (56)$$

Here $\Delta\theta_{a,b}$ is given by Eq. (40), and the largest of the four possible values of η must be used.

By Eq. (44) the voltage for a given pulse varies as $W + d$, so to obtain no interception of the zero-slope beam we have, at cut-off, $V_o \propto (2 + \eta)d$. Had the zero-shape beam not been displaced, we would have $W = d$ and the voltage (V'_o) would vary only as $2d$. Hence the ratio of the voltages, with and without displacement, is

$$V_o/V'_o = 1 + \eta/2. \tag{57}$$

THE DIAGONAL BEAM

It does not seem to have been realized earlier that there is an entrance phase for which ions, on leaving the chopper assembly, have a displacement and slope such that the full intensity beam passes diagonally through the center of the slit, unfortunately with this finite slope. (See Figure 2.) This beam exists in addition to that with zero slope and occurs at a slightly different time. By Eq. (33) we have $x_J = KE_oH$, and this will vanish, irrespective of E_o, when H, as given by Eq. (34), is zero. This condition yields for the input phase θ_{10J} the expression

$$\tan\theta_{10J} = \frac{-m - p(J - r)\omega/\beta c}{n + q(J - r)\omega/\beta c}, \tag{58}$$

the subscript $10J$ denoting the entrance phase for which there is zero displacement at J. The slope of this full intensity beam is given by an expression similar to Eq. (49) but wherein θ_{1co} is replaced by θ_{10J}. The diagonal and cut-off slopes will be equal when we have

$$p\cos\theta_{10J} + q\sin\theta_{10J} = p\cos(\theta_{10v} \pm \Delta\theta_{a,b}) + q\sin(\theta_{10v} \pm \Delta\theta_{a,b}). \tag{59}$$

This can be evaluated for any particular set of parameters to determine a critical $\Delta\theta$ at which the slopes are equal. When $\Delta\theta_{a,b} < \Delta\theta_{\text{crit}}$, the unfortunate condition arises that the fully passed diagonal beam has a greater slope than the vanishing intensity beam at cut-off. Since the possible values of the input parameters are infinite in number, no general tendencies can be quoted. However, if we idealize by assuming no fringing fields, it can be shown that this troublesome situation occurs only for very short pulses when ϕ is large and J/S is small.

"MAGIC" ϕ

As has been stressed, a finite value of x_4 means that part of the zero-slope beam will be intercepted unless the slit be wider than the beam. Further, even if x_4 is small it can be troublesome, since the separation of the two parallel beams (occurring half a cycle apart) can be amplified[2] by the optical properties of a downstream accelerator. If this is intolerable, two pairs of deflecting plates, with opposite and constant potential differences across their gaps, can be placed immediately after the chopper, so as totally to eliminate one beam and bring the other back, without slope, onto the midplane.[2]

Fortunately we need not accept the necessity of a finite displacement of the zero-slope beam. By setting Eq. (23) (for v_4) equal to zero we have obtained Eq. (25), giving $\tan\theta_{10v}$, the entry phase that produces zero slope at the exit from the final ramp. Similarly we now set Eq. (24) (for x_4) equal to zero and obtain an expression for the entry phase that gives zero displacement at the exit:

$$\tan\theta_{10x} = \frac{m}{-n} = \frac{C\cos\phi + D\sin\phi + (\phi\sin\varepsilon)/\varepsilon + 2(1 - \cos\varepsilon)/\varepsilon}{-D\cos\phi + C\sin\phi + \phi(1 - \cos\varepsilon)/\varepsilon - (2\sin\varepsilon)/\varepsilon + 1}. \tag{60}$$

Clearly there must be associated values of ε and ϕ which simultaneously will yield the same value for Eq. (25) as for Eq. (60); that is, there is an entry phase θ_{10vx} which will cause the *zero-slope beam also to have zero displacement*. For convenience we use the word "magic" to identify such particular combinations of ε and ϕ. Equating Eqs. (25) and (60) unfortunately yields an expression which cannot be solved analytically, so a graphical method has been used. For a chosen ε and a series of values of ϕ, θ_1 was plotted as a function of ϕ for both Eqs. (25) and (60); the intersections of the curves give the entry phases, θ_{10vx}, that satisfy both. This process was repeated for a different ε and so on. Unless plotted on an impractically large scale, the critical values of ε and ϕ cannot be read with precision, so subsequently ϕ was varied, in small steps around the approximate values, until θ_{10v} and θ_{10x} agreed to 1 or 2 microradians, for over 1000 values of ϕ_{magic}.

The result of these calculations is shown in Figures 3–8, which display the first six of an infinite number of branches of magic ϕ plotted against ε up to $\varepsilon = 40$. In order to permit evaluation of $V_0 T$ from Eq. (44), μ and ν are also shown in these figures, as calculated from Eqs. (45) and (46), wherein $\theta_{10\nu}$ has been replaced by $\theta_{10\nu x}$. Figures 9 and 10 extend the data up to $\varepsilon = 80$; in this range μ and ν differ so slightly, from branch to branch, that a single set of curves for these quantities is adequate, as is shown in Figure 11. The simultaneous solutions of Eqs. (25) and (60) yield $\tan \theta_{10\nu x}$ so there is necessarily an ambiguity of π radians in the value of this angle; i.e., there are always two associated magic entrance phases, π radians apart. Since μ and ν both depend on $\theta_{10\nu x}$, a corresponding ambiguity in the signs of μ and ν also exists. Fortunately these signs change together, so that only one set of values need be plotted, since we require only the absolute value of $V_0 T$.

It is regretable that journal size prevents plotting the curves on a scale adequate to specify magic ϕ accurately. Nevertheless, with an approximation read from the curves, it is no great task to obtain, by varying ϕ, accurate values of ϕ and of $\theta_{10\nu x}$ for a given ε with the aid of a programmed calculator such as the Hewlett-Packard 65. (Equations (25) and (60) can be put on a single magnetic card.) Computation of higher order branches is facilitated by the observation that, at any ε, the successive values of magic ϕ are increased approximately by 2π. The values of μ and ν are not critical and may be read directly from the curves.

Those values of ε associated with negative μ and a maximum of positive ν are optimal in yielding least $V_0 T$. We note that $|\mu|$ rises with increasing ε; this is fortunate since ε increases with the lowered speed of heavier ions (for constant accelerating voltage) and the larger $|\mu|$ helps to counter the presence of N in the numerator of Eq. (44) for $V_0 T$. For a particular ion ε will rise if G is increased (as may be required for ultra-short pulses) but this gain must be balanced against the reduction of the lever arm $J - 7G$ and the appearance of G in the numerator of Eq. (44).

The anticipated ideal chopper, introducing no slope at cut-off, because of finite μ and zero ν, turns out to be a delusion, at least when the chopper is magic, since, as seen in Figures 3–11, when ν is zero there is an abrupt change in sign of μ, which must therefore pass through zero. This may be seen analytically as follows. By Eq. (25) we have $\tan \theta_{10\nu} = p/-q$ and by Eq. (60) it is seen that $\tan \theta_{10x} = m/-n$. For a magic chopper these entry phases are equal so it follows that

$$n = mq/p. \tag{61}$$

Now by Eq. (46) when $\nu = 0$ we obtain $\sigma = q\kappa/p$ and using this in Eq. (45) for μ gives us $\mu = n\kappa - mq\kappa/p = 0$. Nevertheless it is still true that a finite x_4 (associated with finite μ) will give cut-off with lesser slope as ν approaches zero, although the required V_0 may be prohibitive except with small mass and low frequency.

It must be emphasized that magic ϕ does not occur at a cusp of any curve, so that slight departure from such an optimal value is reflected only linearly in performance. Since $\phi = \omega S/\beta c$, "tuning" to make ϕ become magic may be accomplished by changing any of these parameters. The frequency seems least flexible (and indeed may be prescribed by other considerations) but a small change in ion speed is readily obtained and it does not appear impractical to make a chopper of variable length by the use of two pairs of wedge-shaped plates, one pair being movable. An adjustable gap is also within reason, in order to afford independent control of $\varepsilon = 7G\omega/\beta c$. Any change in the chopper's capacitance will, of course, require alteration of the associated inductance, if the frequency is to be kept constant.

The values of μ and ν are essentially independent of branch number for $\varepsilon > 6$. Different branches may be used to alter ϕ and hence S, so that with a variety of ions (all accelerated through the same potential drop) the chopper can be kept within the bounds of a unit adjustable in length and gap over modest ranges. It is desirable to choose the various parameters to be optimal for the heaviest ion and the shortest pulse contemplated, and to accept less favorable conditions for the lighter particles.

While investigating choppers that were assumed to have no fringing fields, the author had become aware of the properties of magic ϕ, and because a predicted value ($\phi = 0$) implied an absurdity (a chopper of zero length) it was believed that the minimum magic ϕ, with $\varepsilon = 0$, was 8.98 radians, as may be seen in Branch 2, Figure 4. Consequently for the realistic case of finite ε, the emergence of Branch 1, Figure 3, was a welcome surprise, since it shows that magic choppers can be made with considerably shorter lengths. Note that $\phi = \pi$ is magic at certain specific values of ε. The first six useful instances, for which μ is negative and ν is positive (though unfortunately not at a maximum) are listed in Table I, which also gives the entrance

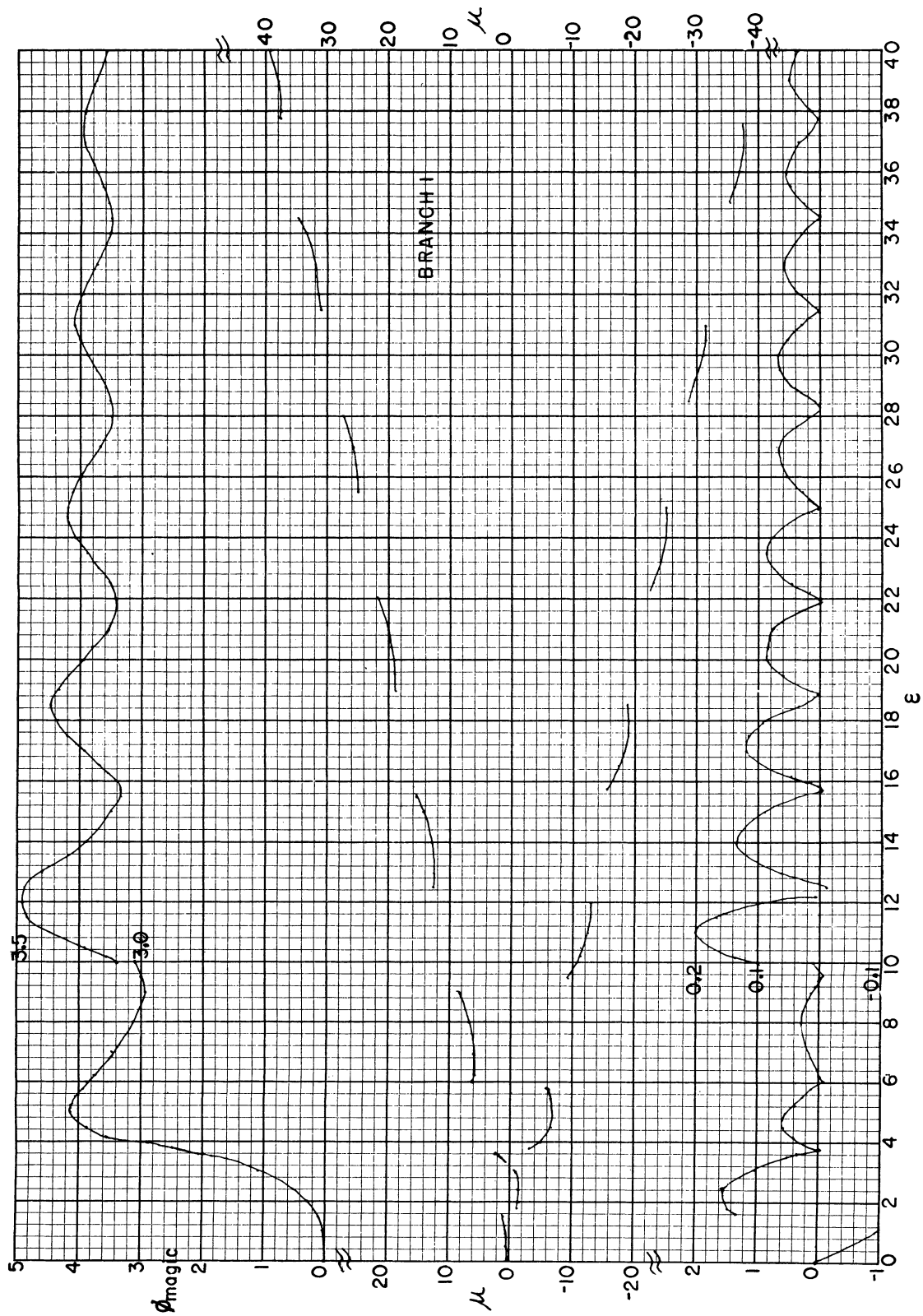

FIGURE 3 Branch 1 of magic chopper angular length $\phi = \omega S/\beta c$ and the quantities μ and ν as functions of the fringe field angular length $\varepsilon = 7G\omega/\beta c$.

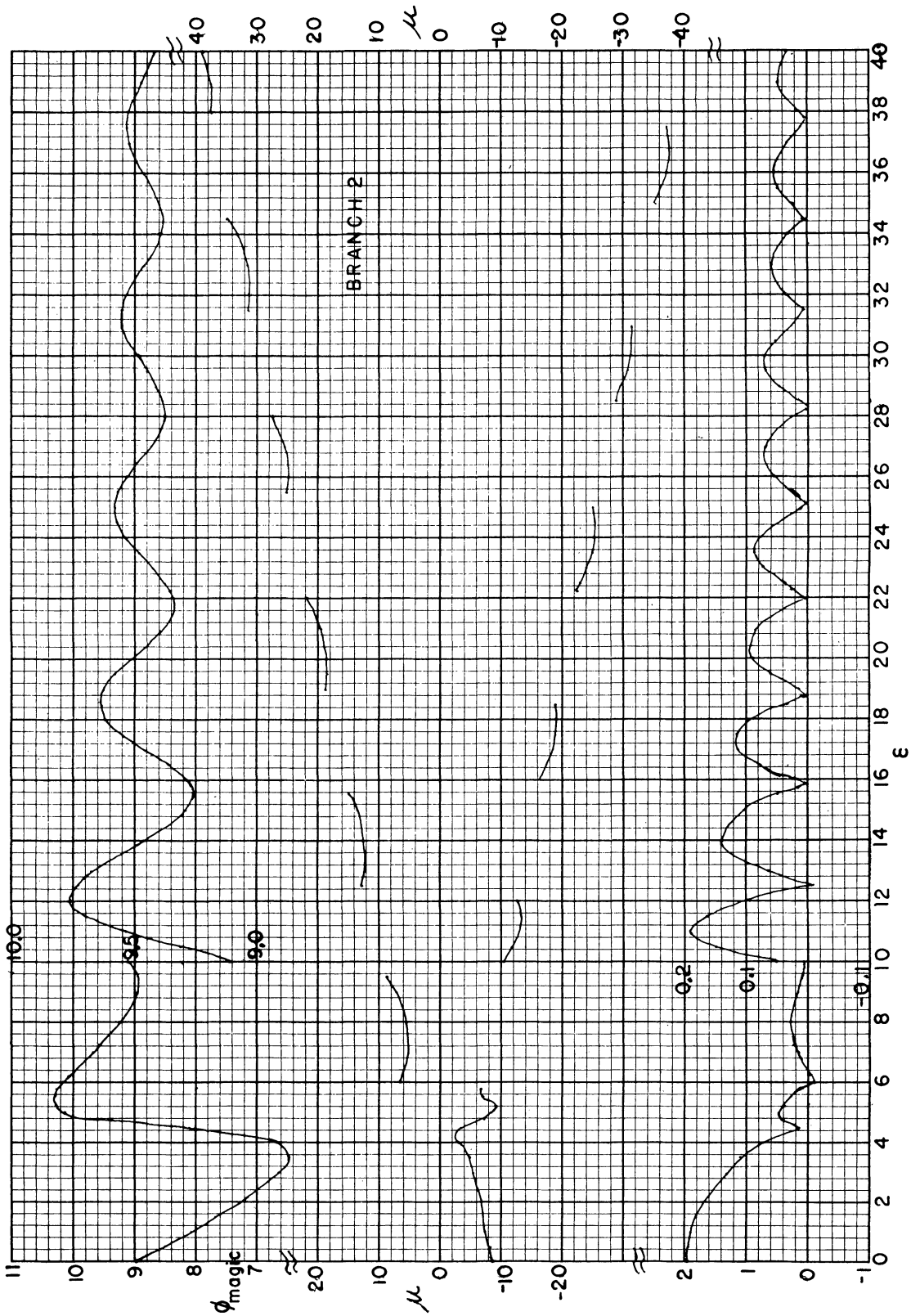

FIGURE 4 Branch 2. (See note added in proof for corrections at $\varepsilon < 1$.)

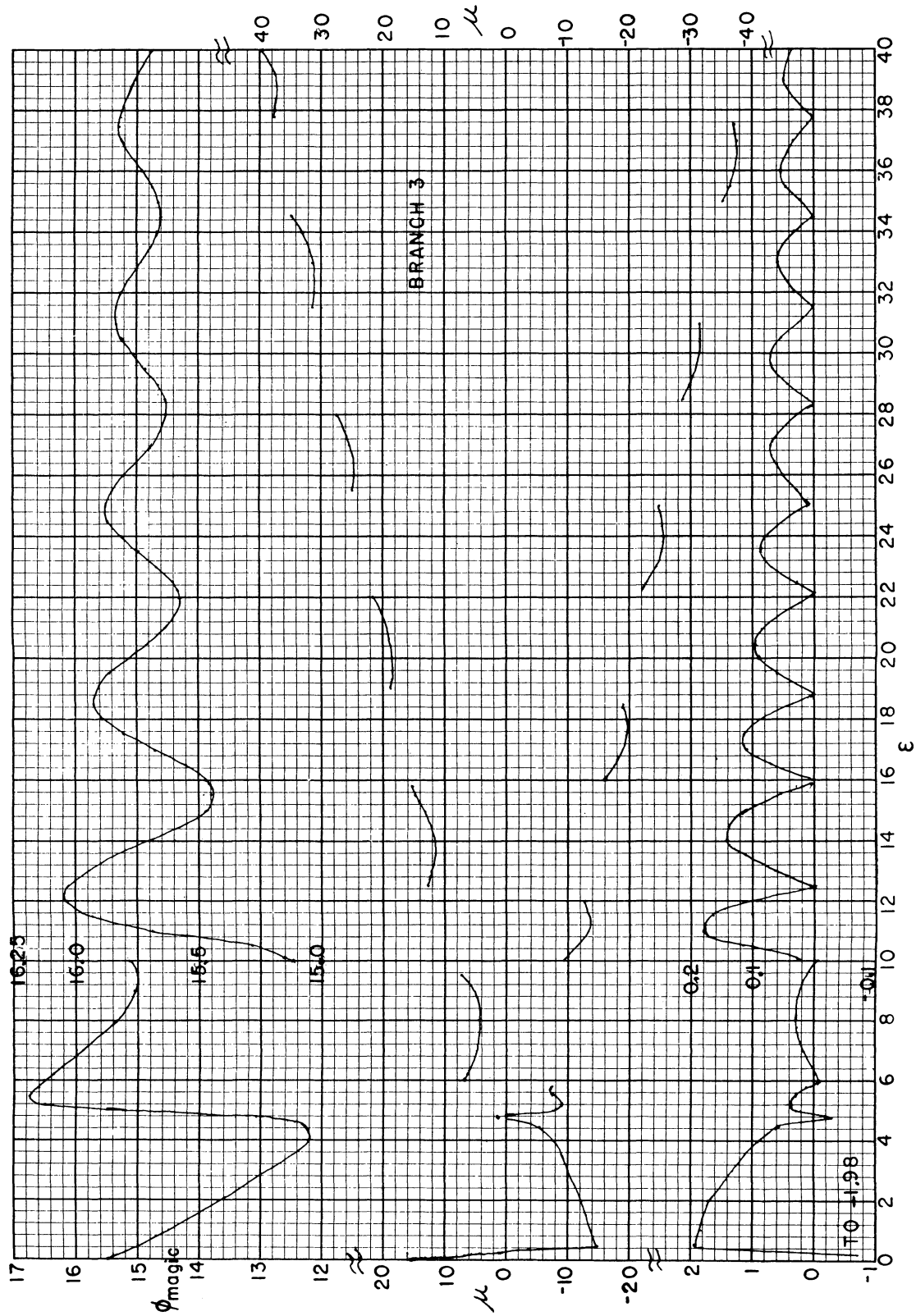

FIGURE 5 Branch 3. (See note added in proof for corrections at $\varepsilon < 1$.)

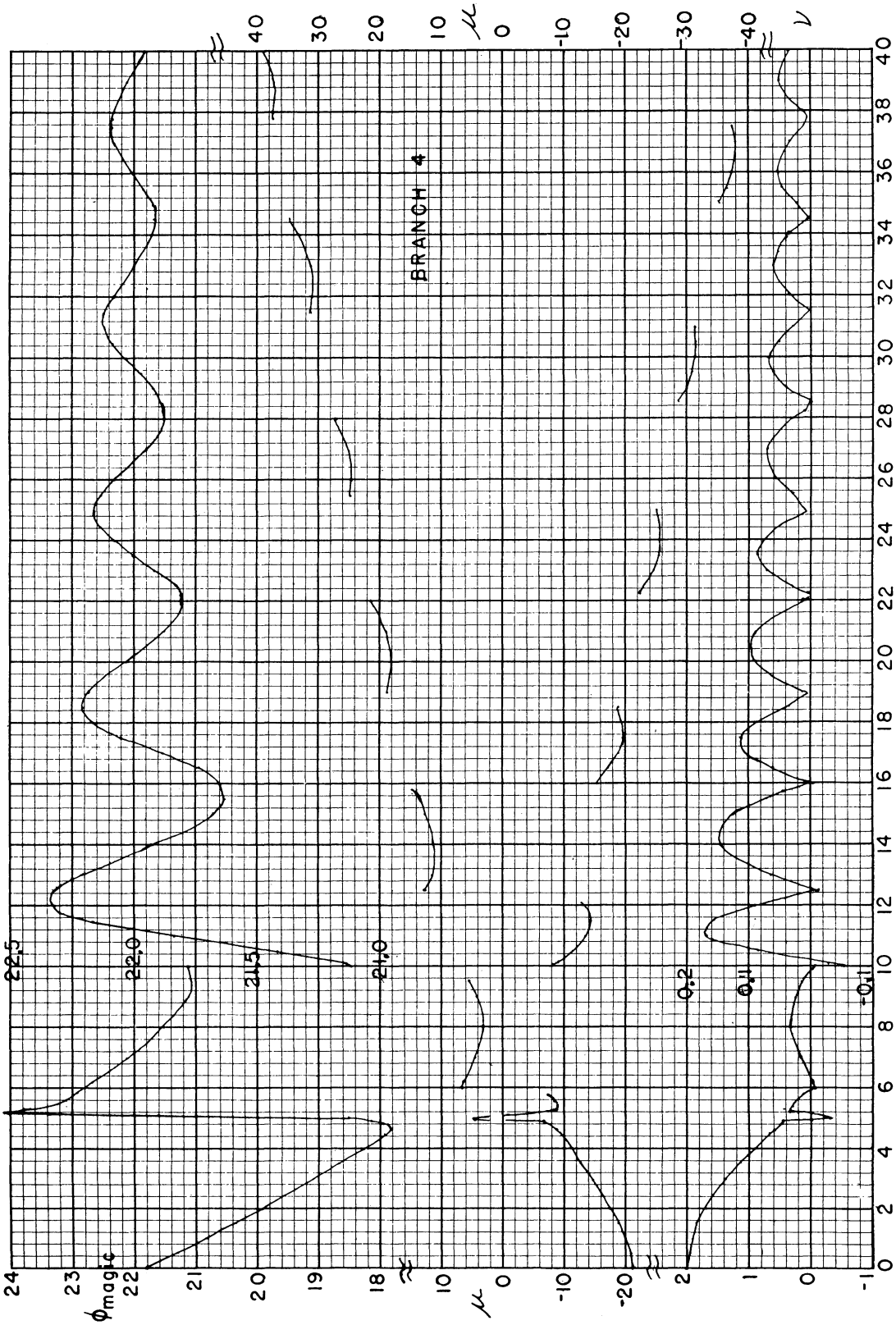

FIGURE 6 Branch 4. (See note added in proof for corrections at $\varepsilon < 1$.)

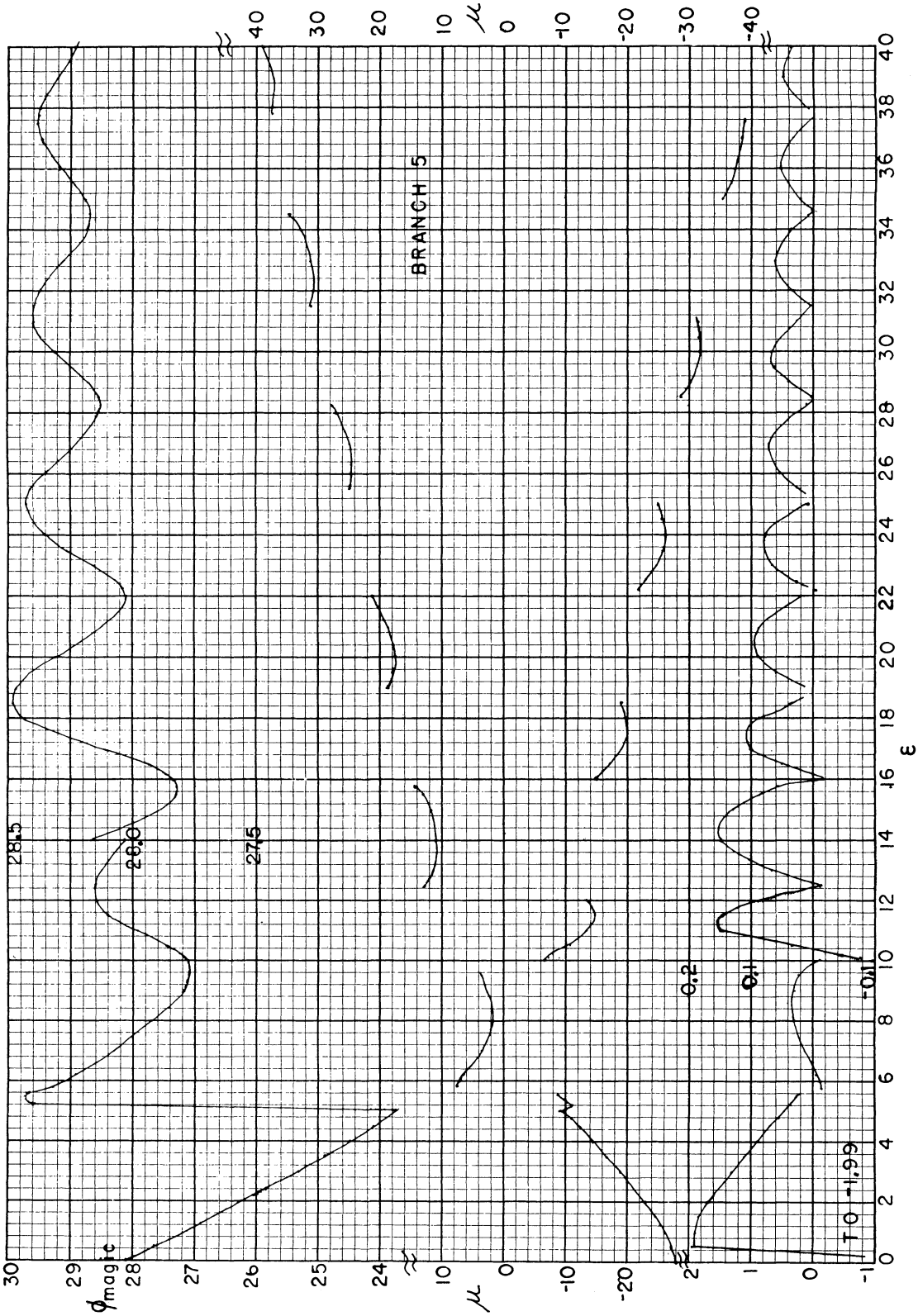

FIGURE 7 Branch 5. (See note added in proof for corrections at $\varepsilon < 1$.)

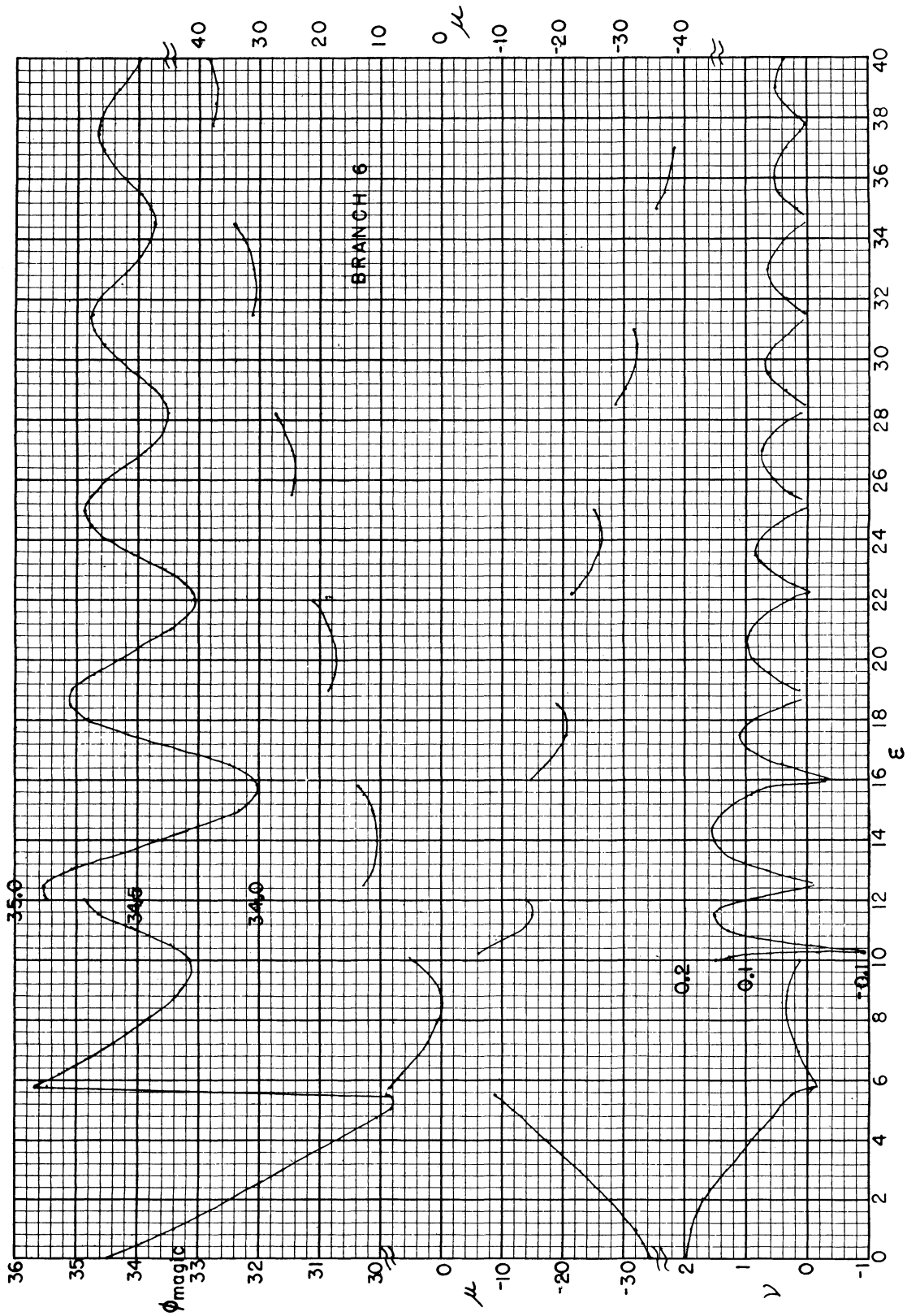

FIGURE 8 Branch 6. (See note added in proof for corrections at $\varepsilon < 1$.)

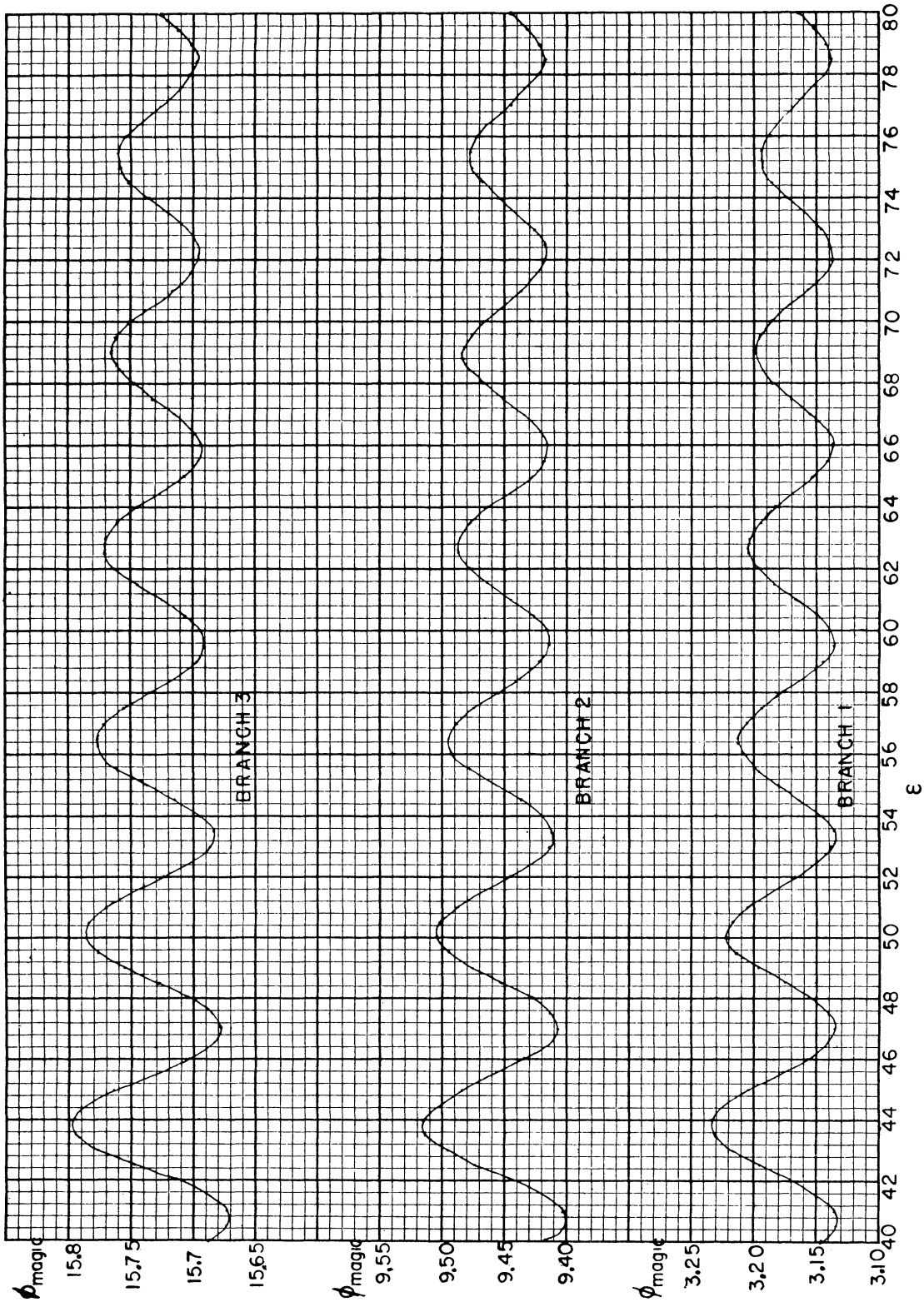

FIGURE 9 Branches 1, 2, 3 at larger ε

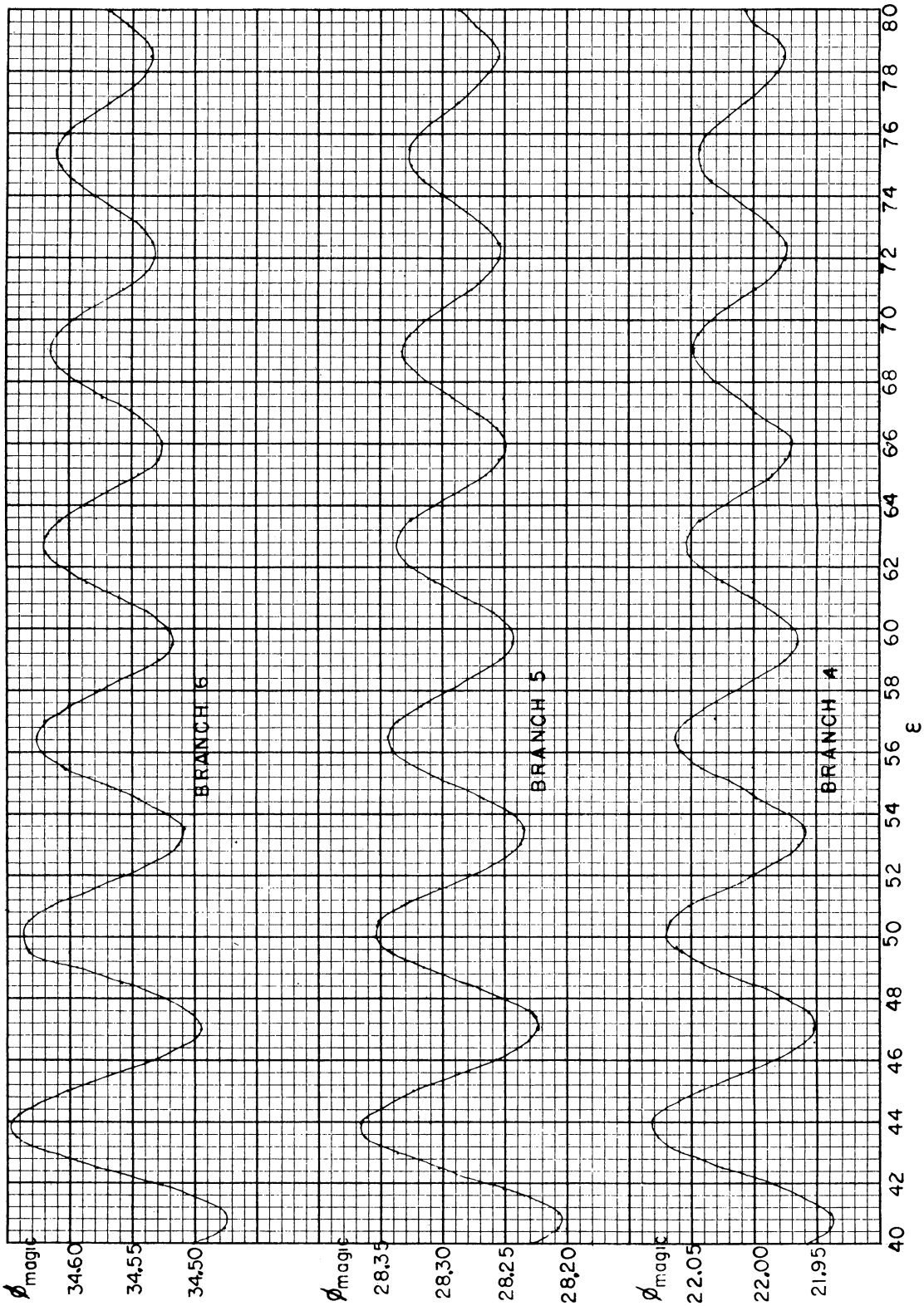

FIGURE 10 Branches 4, 5, 6 at larger ε.

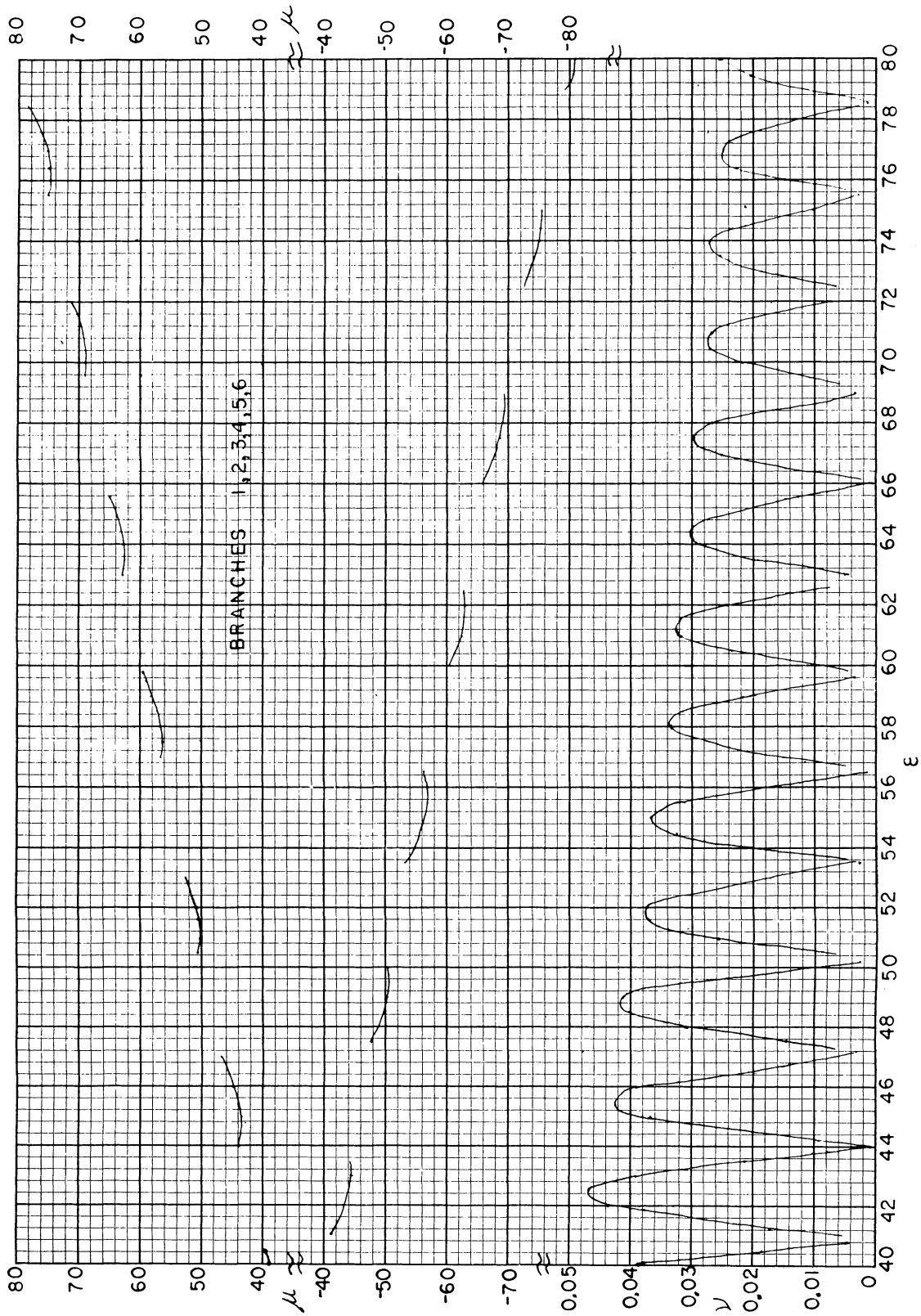

FIGURE 11 μ and ν for Branches 1–6 at larger ε.

phase angle as well as μ, ν and the largest interior displacement. This latter is needed in finding the required gap and the minimum pulse.

TABLE I

Parameters for magic $\phi = \pi$.

ε (rad)	$\theta_{10\nu x}$ (rad)	μ	ν	x_{max}/KE_o
4.092029	0.620360	−5.53	0.398	−2.397
10.17345	0.822124	−11.06	0.134	−2.134
16.350445	0.928315	−17.06	0.073	−2.073
22.56465	0.997295	−23.18	0.048	−2.048
28.79816	1.046971	−29.35	0.035	−2.035
35.04310	1.085115	−35.55	0.027	−2.027

It is interesting to note that for these cases the sum of ε, $\theta_{10\nu x}$ and ϕ equals $\pi/2$ multiplied by 5, 9, 13, 17, 21 and 25.

NO DIAGONAL BEAM WITH MAGIC ϕ

Equation 25 has shown that $\tan\theta_{10\nu} = p/-q$, and when Eq. (58) for $\tan\theta_{10J}$ is multiplied by pq/pq it becomes

$$\tan\theta_{10J} = \tan\theta_{10\nu}\left(\frac{mq/p + q(J-r)\omega/\beta c}{n + q(J-r)\omega/\beta c}\right). \quad (62)$$

But for a magic chopper we have $n = mq/p$ by Eq. (61), so the diagonal beam has the same entry phase as that for which the output slope is zero. The diagonal beam no longer exists.

$\Delta\theta_a = \Delta\theta_b$ WITH MAGIC ϕ

Equation (40) reads $\Delta\theta_{a,b} = \omega T/2 \pm X/Y$ and if we multiply the last term by KE_o/KE_o its numerator becomes [by use of Eqs. (36), (24) and (23)]

$$XKE_o = x_4 + v_4(J-r)/\beta c.$$

But for magic ϕ both x_4 and v_4 are zero and hence so also is X. Therefore

$$\Delta\theta_a = \Delta\theta_b = \omega T/2. \quad (63)$$

This is in accord with expectation since the zero slope beam lies on the axis and equal changes in entrance phase will cause equal deflections for cut-off. As a result of Eq. (63) we see from Eq. (50) that the two intercepted beams have slopes of equal absolute value.

$W = d$ WITH MAGIC ϕ

Although this is intuitively obvious, an analytic demonstration is at hand. We return to Eqs. (55) and (56) for W/d and note that the numerator of Eq. (56) is $m\kappa + n\sigma$, which by Eq. (24) is proportional to x_4. But that is zero with magic ϕ, so it follows that $W = d$; the slit need be no wider than the beam diameter.

MINIMUM GAP AND PULSE WITH MAGIC ϕ

The optimal values of ε (occurring when μ is negative and ν is at a positive peak) are essentially identical for all branches when $\varepsilon > 10$, as is seen in Figs. 3–11. The points in the upper half of Figure 12 give the greatest internal displacements, x_{max}/KE_o, for the zero slope zero displacement beam. The lower half shows the corresponding values of $\theta_{10\nu x}$; this information is needed in deciding whether $\Delta\theta(=\omega T/2)$ is negligible compared with $\theta_{10\nu x}$ when calculating G_{min} and T_{min}. The lines between the points, in both parts of the figure, are simply to guide the eye and do not indicate values at intermediate ε.

THE ANALYSIS FOR NEGLIGIBLE FRINGING FIELDS. $\varepsilon = 0$.

Since $(\sin\varepsilon)/\varepsilon$ and $(1-\cos\varepsilon)/\varepsilon$ are indeterminate when $\varepsilon = 0$, these functions must be expanded to two terms before we set $\varepsilon = 0$. Relevant results are given in Table II;

TABLE II

Function values for $\varepsilon = 0$

$(\sin\varepsilon)/\varepsilon =$	1	$p = 1 - \cos\phi$
$(1-\cos\varepsilon)/\varepsilon =$	0	$q = \sin\phi$
$A =$	0	$m = \phi - \sin\phi$
$B =$	0	$n = 1 - \cos\phi$
$C =$	0	$\mu = \phi\sin\frac{1}{2}\phi$
$D =$	−1	$\nu = -2\sin\frac{1}{2}\phi$
$A/\varepsilon =$	−1	$\sigma = -\sin\frac{1}{2}\phi$
$B/\varepsilon =$	0	$\kappa = \cos\frac{1}{2}\phi$

The calculations for μ, ν, σ and κ involve the trigonometric identities for $\tan\frac{1}{2}\phi$ and Eqs. (27), (28) and (66).

At entry to the chopper, Eqs. (7) and (8) show that v_2 and x_2 are zero. At exit from the chopper,

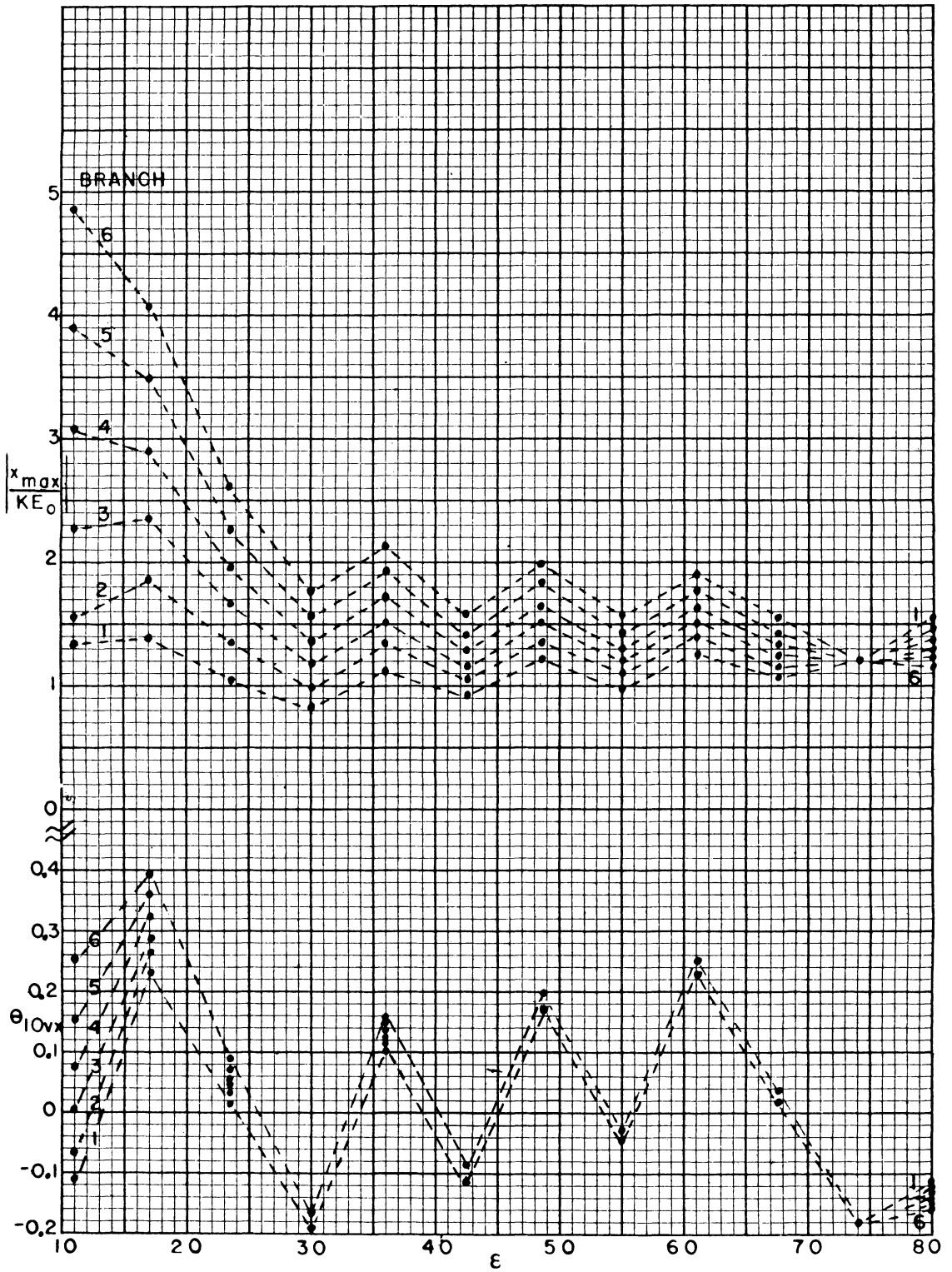

FIGURE 12 Maximum interior displacement and entrance phase for optimal magic choppers as function of ε. Dashed lines do not indicate values at intermediate ε.

Eqs. (12), (23), (13) and (24) become

$$v_3 = v_4 = KE_o\omega[\cos\theta_1(1 - \cos\phi) + \sin\theta_1 \sin\phi] \quad (64)$$

$$x_3 = x_4 = KE_o[\cos\theta_1(\phi - \sin\phi) + \sin\theta_1(1 - \cos\phi)]. \quad (65)$$

Equation (25) is now

$$\tan\theta_{10v} = p/-q = (1 - \cos\phi)/(-\sin\phi) = -\tan\tfrac{1}{2}\phi$$

so the entry phase for zero slope at emergence is given by

$$\theta_{10v} = -\phi/2. \quad (66)$$

This is a well known[2] relation for $\varepsilon = 0$; the ions enter at such a phase that the field passes through zero when the particles are at the chopper's midpoint. Hence an upward deflection in the first half is cancelled by a downward bend in the second, so the emergent path is parallel to that at entry (i.e., it has zero slope) but it is displaced upward. The simple relation of Eq. (66) does not hold when ε is finite.

When Eq. (66) is used for θ_1 in Eq. (65), we find that

$$x_3 = x_4 = KE_o[\phi \cos\tfrac{1}{2}\phi - 2\sin\tfrac{1}{2}\phi] \quad (67)$$

and if we also now demand that Eq. (67) must vanish, the criterion for magic ϕ (zero slope and displacement at the exit) is found to be

$$\phi = 2\tan\tfrac{1}{2}\phi. \quad (68)$$

The first 18 values of ϕ that satisfy this are given in Table III:

TABLE III

Magic ϕ (radians) for $\varepsilon = 0$.

0	40.742606	78.488865
8.986819	47.038905	84.775827
15.450504	53.332109	91.062268
21.808243	59.623219	97.348288
28.132387	65.912778	103.633965
34.441510	72.201244	109.919356

The first six of these are recognized as the $\varepsilon = 0$ values of ϕ in Figures 3–8. The differences between successive entries in this table range progressively from 2.860π to 2.00070π.

When $\varepsilon = 0$, the fringe field length r is zero, and the use of Table II turns Eq. (44) into

$$V_o T = \frac{1.04 \times 10^{-12} G\omega N(W + d)}{\phi \sin\frac{1}{2}\phi(1 + 2J/S)}. \quad (69)$$

This is the same expression (although in different notation) as that given in Eq. (A5) of Ref. 2, wherein fringing fields were neglected. The factor $\sin\frac{1}{2}\phi$ has been a compelling argument for choosing $\phi = \pi$, for then $V_o T$ is a minimum.

NO DIAGONAL BEAM WITH $\varepsilon = 0$ AND MAGIC ϕ

The use of Table II in Eq. (58) (now with $r = 0$) gives

$$\tan\theta_{10J} = \frac{-\phi + \sin\phi - (1 - \cos\phi)J\omega/\beta c}{1 - \cos\phi + \sin\phi\, J\omega/\beta c}. \quad (70)$$

In only the numerator of this use Eq. (68) and the identities $\sin\phi = (1 + \cos\phi)\tan\frac{1}{2}\phi$ and $1 - \cos\phi = \sin\phi \tan\frac{1}{2}\phi$, to find that Eq. (70) becomes $\tan\theta_{10J} = -\tan\frac{1}{2}\phi$. By Eq. (66) $-\frac{1}{2}\phi$ is equal to the entrance phase for zero slope at the exit, so the "diagonal" beam now no longer exists. This is the same result as was found when ε was finite and ϕ was magic.

$\Delta\theta_a = \Delta\theta_b$ WITH $\varepsilon = 0$ AND MAGIC ϕ

Using the expressions for σ, κ, m and n of Table II and the identities for $\tan\frac{1}{2}\phi$ we find that

$$m\kappa + n\sigma = \phi\cos\tfrac{1}{2}\phi - 2\sin\tfrac{1}{2}\phi$$
$$p\kappa + q\sigma = 0$$
$$m\sigma - n\kappa = -\phi\sin\tfrac{1}{2}\phi$$
$$p\sigma - q\kappa = -2\sin\tfrac{1}{2}\phi.$$

Hence Eqs. (36) and (37) become

$$X = \phi\cos\tfrac{1}{2}\phi - 2\sin\tfrac{1}{2}\phi \quad (71)$$

$$Y = -\phi\sin\tfrac{1}{2}\phi - (2\phi J/S)\sin\tfrac{1}{2}\phi, \quad (72)$$

the latter since $\omega/\beta c = \phi/S$. It follows from Eq. (40) that

$$\Delta\theta_{a,b} = \frac{1}{2}\left[\omega T \mp \frac{(2\phi/\tan 1/2\phi) - 4}{\phi(1 + 2J/S)}\right]. \quad (73)$$

For $\varepsilon = 0$ and magic ϕ we have $\phi = 2\tan\frac{1}{2}\phi$ so that

$$\Delta\theta_a = \Delta\theta_b = \omega T/2 \quad (74)$$

as expected.

REFERENCES

1. E. Weber, *Electromagnetic Theory*, p. 335, Dover, 1965.
2. C. M. Turner and S. D. Bloom, *Rev. Sci. Instr.*, **29**, 480 (1958).

Note added in proof. Not shown in Figures 3 to 8 are favorable conditions for V_0T occurring in Branches 1–6 for certain ranges of small ε, wherein μ is large and positive while ν is large and negative. These regions are followed by sudden drops to equally large negative μ (which thereafter becomes less negative) while ν rises abruptly to positive values (subsequently falling slowly). The first of these optimal regions are described approximately in Table IV.

Note that μ increases with Branch number and that the range of favorable ε becomes progressively smaller.

Xeroxed sheets giving ε, ϕ_{magic}, θ_{10vx}, μ and ν for all six branches in the range $\varepsilon = 0$ to 5 (from which curves may be plotted for interpolation) are available on request.

TABLE IV

μ, ν and ϕ_{magic} at small ε.

Branch	ε range		μ	ν	ϕ_{magic} range	
1	0	1.50	0 to 0.97	0 to −1.3	0	0.1167
2	0.001	0.40	8.6	−2	8.9858	8.5984
3	0	0.25	15	−2	15.4505	15.2031
4	0.001	0.15	21.6	−2	21.8082	21.6589
5	0	0.10	28	−2	28.1323	28.0326
6	0.001	0.10	34	−2	34.4405	34.3417